Manipulating the one-dimensional topological edge state of Bi bilayer nanoribbons via magnetic orientation and electric field

Jeongwoo Kim and Ruqian Wu

Phys. Rev. B **97**, 115151 — Published 26 March 2018

DOI: 10.1103/PhysRevB.97.115151

Manipulating one-dimensional topological edge state of Bi-bilayer nanoribbons via magnetic orientation and electric field

Jeongwoo Kim, & Ruqian Wu*

Department of Physics and Astronomy, University of California, Irvine, California 92697, USA

Abstract:

Despite the superiority of two-dimensional (2D) topological insulators (TIs) over their three-dimensional (3D) counterparts in various aspects and the essential distinction between them in structural symmetry, the variation of the topological 1D edge states upon magnetic interaction and their application for spintronic devices have not been sufficiently illuminated. Here, we reveal that 1D edge states of 2D TI have a unique magnetic response never observed in 2D surface states of 3D TI, and using this exotic nature we propose a new way to utilize the spin-polarized channel for spintronic applications. We investigate the effects of width and magnetic decoration on the 1D topological edge state of Bi-bilayer nanoribbons (BNRs). Through the Zak phase, we find that the zero-energy states are enforced at the magnetic domain boundaries in the Cr-decorated BNR and directly examine their robustness using short-range magnetic domain structures. We also demonstrate that 1D edge states of BNRs can be selectively and reversibly controlled by the combination of magnetic reorientation and electric field without compromising their structural integrity. Our work provides a fundamental understanding of 1D topological edge states, and shows the opportunity of using these features in spintronic devices.

Email: wur@uci.edu

PACS numbers: 75.70.Ak, 75.50.Pp, 75.25.-j, 73.20.At

Ⅰ. INTRODUCTION

Since graphene inaugurated an era of two-dimensional (2D) materials in a decade ago [1], extensive efforts have been dedicated to finding innovative 2D systems that can host new quantum phenomena [2-6]. One plausible example is the realization of the quantum spin Hall effect [7, 8] in HgTe/CdTe quantum wells [9, 10], which are now viewed as prototypical 2D topological insulators (TIs). Ideally, the one-dimensional (1D) chiral edge states of 2D TIs are immune to backscattering by local disorders due to the spin-momentum locking feature [11]. Especially, 2D TIs have advantages over their three-dimensional (3D) counterparts in terms of applicability and controllability [12-16]. The Fermi level of a 2D TI can be easily tuned by gate voltage, and its electronic structure can be also manipulated via structural deformation and chemical modification [15-17]. Among various types of 2D TIs, Bi bilayer ultrathin films are the most promising candidate for practical applications [18-24]. Bi bilayers have been successfully grown on a few substrates and shown the presence of edge-localized states in experiments [25-28]. Recently, a monolayer bismuthene [29], one of chemically modified variations of Bi-bilayer, was also realized on a SiC substrate as theoretically predicted [30-32]. Obviously, fundamental studies of 2D TIs such as ultrathin Bi films and ribbons are of great importance for the discovery of new science and for the development of excellent spintronics materials.

Although tremendous experimental achievements have been made for understanding 2D TIs in various aspects, much less attention has been dedicated to the magnetic effect on their topological edge states. Since a variety of magnetic configurations can be constructed through the proximity effect of magnetic substrates and edge decorations [33-37], it is intriguing to investigate how the topological states of a 2D TI can be manipulated. The magnetic domain boundaries in a 1D chain can be extremely thin due to the large magnetic

anisotropy and missing neighbors. This provides a nice playground for examining the interplay between magnetic ordering, bias, and lattice strain on the topological, magnetic, and electronic properties of low-dimensional materials. Note that the effective model Hamiltonian describing 1D edge states of 2D TIs [19] is fundamentally inequivalent to that describing the surface states of 3D TIs [38], and the response of the topological 1D edge states to magnetic interaction is a new issue and should therefore be separately discussed [39].

Here, we investigate the modification of the electronic structure of 1D topological edge states caused by edge magnetism in Cr-decorated Bi-bilayer nanoribbons (BNR). Based on density functional theory (DFT) calculations, we study how the addition of exchange interaction into 1D edge states affects the topology of BNR by varying the size of BNR and magnetic configurations. We show the zero-energy state is enforced at the magnetic domain boundary in the Cr-decorated BNR through the Zak phase calculation. We also examine the appearance of the nontrivial state by constructing magnetic interfaces in a large supercell. We find an edge-selective conduction in BNRs can be realized via a combined operation with edge magnetism and external electric field. Our results provide a useful guideline to engineer low-dimensional quantum phenomena for the exploitation of 2D TIs in spintronic devices.

Ⅱ. METHOD

Our DFT calculations are performed using the projected augmented plane-wave method [40, 41] as implemented in the Vienna *ab initio* simulation package (VASP) [42]. The Perdew-Burke-Ernzerhof functional of the generalized gradient approximation is used for the description of exchange-correlation interactions among electrons [43]. BNRs consisting of 40 Bi and 2 Cr atoms in supercells are separated by more than 15 Å in all directions. All BNRs used in our calculations are periodic along the *y*-axis. The spin-orbit coupling term is

included in the self-consistency loops. The energy cutoff for the plane-wave-basis expansion is chosen to be 300 eV. We adopted a 1×15×1 **k**-point grid to sample the essentially 1D Brillouin zone. The positions of all atoms are fully relaxed until total energies are converged to better than 0.1 meV per formula unit. Using the Wannier charge centers calculation [44] as implemented in the QUANTUM ESPRESSO code [45], we calculated the Zak phase according to, $\varphi=\sum_n i\int dk\left\langle u_{nk}\left|\frac{\partial u_{nk}}{\partial k}\right.\right\rangle$ [46], where u_{nk} is the Bloch wave-function and energy of the *n*-th band at a *k*-point.

Ⅲ. RESULT AND DISCUSSIONS

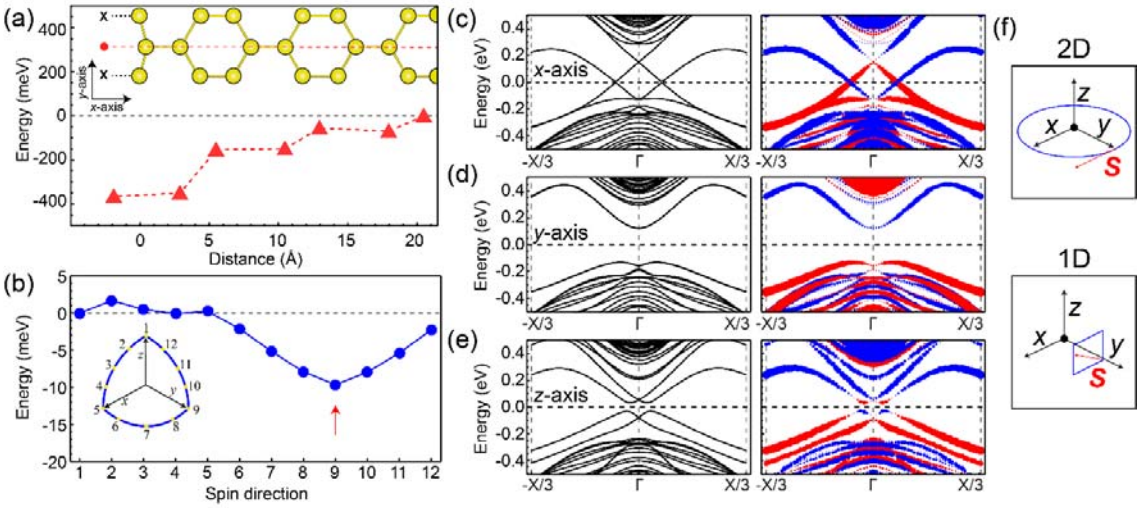

Figure 1 (a) Calculated adsorption energy of Cr atom on BNR along the lateral direction. The innermost hollow-site energy is set to zero. A schematic atomic structure of BNR is shown in the upper part of (a). Red dots and black crosses represent two different Cr-adsorption sites. (b) Calculated total energy of Cr-decorated BNR varying the spin direction of Cr atom. The spin direction represented in the inset is labelled from 1 to 12. Calculated band structure and its spin projection in Cr-decorated BNR with the local magnetic moment aligned along (c) the x-axis, (d) the y-axis, and (e) the z-axis. Spin up (down) states are marked by red (blue) dots. (f) The schematic drawing of the spin(red arrows)-momentum(black arrows) locking for 2D surface states and 1D edge states. The z-direction

and the y-direction magnetizations break the time-reversal symmetry because they are perpendicular to the spin-rotating plane (blue lines) for the 2D and the 1D, respectively.

As the first step for our investigation of the magnetic effect on the edge states, we introduce Cr atoms. Cr atoms prefer to take the edge sites between outermost Bi atoms as marked by the red dot in Fig. 1(a), according to total energies. For example, this geometry is 0.45 eV lower in energy than the case by directly attaching Cr atoms to the outermost Bi atoms as marked by the black crosses in Fig. 1(a). Based on the optimized Cr-decorated BNR structure, we calculated the preferred spin direction of localized Cr magnetic moments. Fig. 1(b) shows that the spin anisotropy energy dose not change much in the *x*-*z* plane and the easy magnetization is along the *y*-axis (red arrow).

One important point is that the electronic structure of BNR is very sensitive to the direction of magnetization of Cr. Unlike the topological surface states of 3D TIs that have only two distinguishable directions, parallel or perpendicular to the surface, the topological edge states of 2D TIs have three distinct spin directions. For the case that magnetization is along the *x*-axis, the linear dispersion of the edge state is preserved even in the presence of the localized magnetic moment [Fig. 1(c)]. The spin-projected band structure indicates that two different Dirac cones are split in the momentum space, which is analogous to the Dirac cone translation induced by the in-plane magnetization for 3D TIs [47]. Due to the spin-momentum locking feature, the spin of topological edge state lies in the *x*-*z* plane as shown in Fig. S1[19, 48] as the momentum direction of the edge state (or the cutting direction) is fixed to the *y*-axis in 1D BNR [Fig. 1(d), inset]. The *x*-direction magnetization does not induce a gap because the spins of the edge states are mostly polarized along the same direction (*x*-direction) by the strong interconnection between the edge state and the edge magnetization [Fig. 1(c)]. When the magnetic moment is aligned along the *y*-axis, the linear bands disappear,

and a wide gap opens near the Fermi level as shown in Fig. 1(d), indicating that the time-reversal symmetry is broken. Since the external field perpendicular to the plane in which the spin of the topological state is rotating [blue lines in the inset of Fig. 1(d)] destroys the time-reversal symmetry, the magnetization pointing along the *y*-direction corresponds to the surface normal direction of the topological 2D surface states.

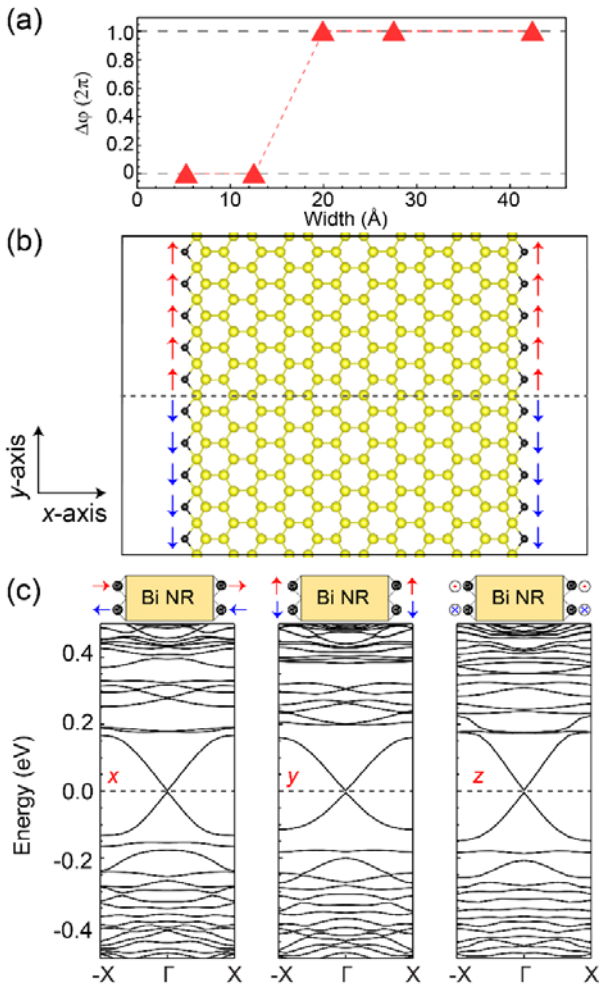

Figure 2 (a) The variation of the Zak phase upon the width (W) of BNR passivated by Cr atoms. The local magnetic moment of Cr atom is parallel or antiparallel to the y-axis. (b) A schematic structure of Cr-decorated BNR (W=42.5 Å) expanded along the y-axis. A (1×10) supercell is used to reproduce the magnetic domain boundary. Yellow balls, Bi; Black balls, Cr. Spin up (down) states are marked by red (blue) arrows. (c) Calculated band structure of the BNR supercell depending on the spin direction. The spin direction is indicated at the top of the panels.

Interestingly, the *z*-direction magnetization generates a new low-energy state that has not been discussed for topological surface states [Fig. 1(e)]. To understand this unique feature, we construct an effective model Hamiltonian which is expressed as $H = \tau\hbar v k_y(\lambda\sigma_x + \sqrt{1-\lambda^2}\sigma_z) + \vec{\mathbf{M}}\cdot\vec{\boldsymbol{\sigma}}$, where v is the Fermi velocity, $\vec{\boldsymbol{\sigma}}$ are the Pauli matrices, and the helicity of Dirac fermions τ is identical to σ_z. $\vec{\mathbf{M}}$ and λ are the magnetic moment and a normalization factor for the σ_x component, respectively. The first term describes the topological edge state with the σ_x and σ_z components and the magnetic exchange effect is represented in the second term of this model Hamiltonian.

For the σ_z component of the edge states, the *z*-direction magnetic moment (M_z) yields a shift of the Dirac point by $M_z\sigma_z$ in the momentum space as already shown in Fig. 1(c), whereas M_z plays as a source of a mass gap for the σ_x component of the edge states. The Dirac cone near the Γ point is dominated by the σ_z component along with a small contribution from the σ_x component (Fig. S1) [48]. Therefore, by combining the translation of the Dirac cone toward the X point and the mass gap at the band crossing point, the W-shape (or M-shape) topological edge state develops around the Γ point [Fig. 1(e)].

To more closely see how magnetism at the edges affects the topological phase of BNR, we investigated the 1D Berry phase also known as the Zak phase in the most stable spin configuration with the *y*-direction magnetization. When the width of BNR is greater than 20 Å, as shown in Fig. 2(a), the Zak phase difference between the spin-up state and the spin-down state reaches a constant: 2π (π per each edge), which means that there is a zero-energy state enforced by the topology at the magnetized edges of BNR as suggested by theory [11]. The sign of a mass (m) of Dirac cone is determined by the direction of the magnetization and the mass should be zero at the magnetic domain wall where the mass should be continuously

changed from $+m$ to $-m$. In other words, at the domain boundary between the spin-up state and the spin-down down state in an expanded supercell, a chiral state is always developed by their topological difference and preserved as long as the magnetic configuration is maintained. To appreciate the robustness of the topological zero energy state, we directly calculate its localization in a 1×10 supercell (43.1 Å along the *y*-axis) as illustrated in Fig. 2(b). Contrary to the conventional perception that the localized zero-energy state develops at the boundary, the topological edge states spreading over the entire edge is restored and the signature of the boundary state is not found near the Fermi level (Fig. S2) [48]. Fig. 2(c) also shows that the sharp Dirac cone is restored at the Γ point by the magnetic domain structure and this recovery of the linear dispersion is independent of the local spin direction. Based on our findings, we hypothesize that the topological edge state is rather delocalized and sense the averaged magnetization in the supercell. As a result, the magnetization effect on the edge state vanishes when adjacent magnetic domains are exactly antiparallel to each other.

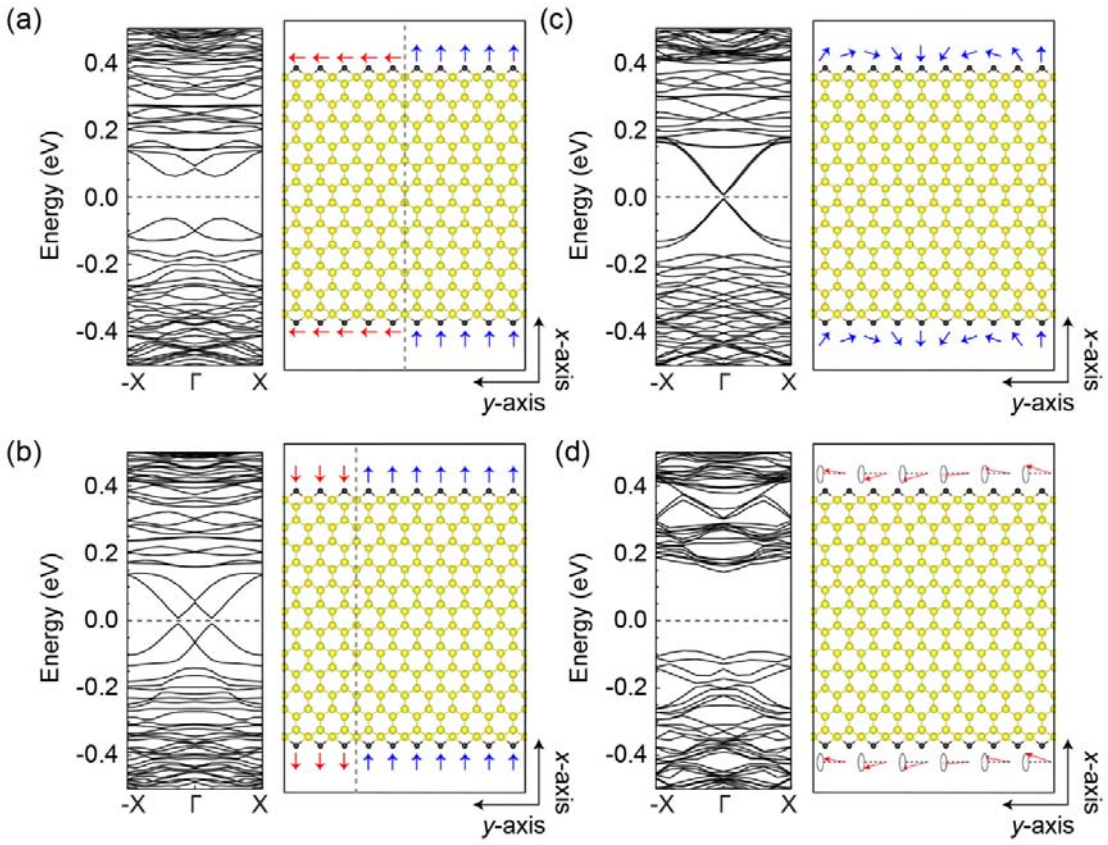

Figure 3 (a)-(d) Calculated band structure (left) and corresponding schematic drawing (right) for various types of magnetic configuration. A domain boundary (a) that two magnetic domains have different magnetic easy axes (x-and y-axis) and (b) that magnetic domain sizes are inequivalent and they are antiparallel (+x and –x). A spin wave excitation (c) that the local spins rotate in the x-y plane and (b) that the local spins precess around the y-axis. Yellow balls, Bi; Black balls, Cr.

To prove our hypothesis, we explored the association of the topological edge state with the magnetic exchange interaction thoroughly by considering a variety of spin domain configurations. When two magnetic domains (*x*-and *y*-axis) whose spin directions are perpendicular to each other are contiguous, the gapped Dirac cones shifts toward the X point and they look like to have band structures of two different magnetic domains in the same plot [Fig. 3(a)]. For example, the mass gap is produced by the *y*-direction magnetization and the Dirac cone shift away from the Γ point is caused by the *x*-direction magnetization. We

also tested the case that the sizes of neighboring domains are inequivalent [Fig. 3(b)]. Due to the diminished net magnetization, the shift of the Dirac point is also decreased compared with the case without a domain boundary (Fig. S3) [48]. Our results imply once again that the net magnetic moment is more important than magnetic patterns in a nanometer scale. We note that, in principle, the 2D topological surface states can show a similar response to a magnetic impurity as the 1D edge state [39, 47].

We also examined how the spin wave excitation affects the electronic structure of Cr-decorated BNR. When spins rotate in the *x*-*y* plane and the net magnetization is constrained at zero as illustrated in Fig. 3(c), the Cr-decorated BNR shows linear bands, very similar to Fig. 2(c). We note that, since the BNR width we are using is not thick enough to eliminate the coupling of two edges and a very small magnetic moment survives, a small energy gap appears in the spin wave case. For the spin precession around the *y*-axis [Fig. 3(d)], BNR becomes an insulator with a band gap of 0.2 eV as also seen in Fig. 1(d) and Fig. S3 [48]. This means that the precession does not change the electronic structure of BNR. Our results for the various configurations confirm that the edge state depends on the averaged magnetization unless its coherence length becomes shorter than the domain size. It is important to point out that we are not able to get the zero-energy state that is supposed to be protected by the topology at the interface. Hence, the topologically protected zero-mode state is not robust in Cr-decorated BNR.

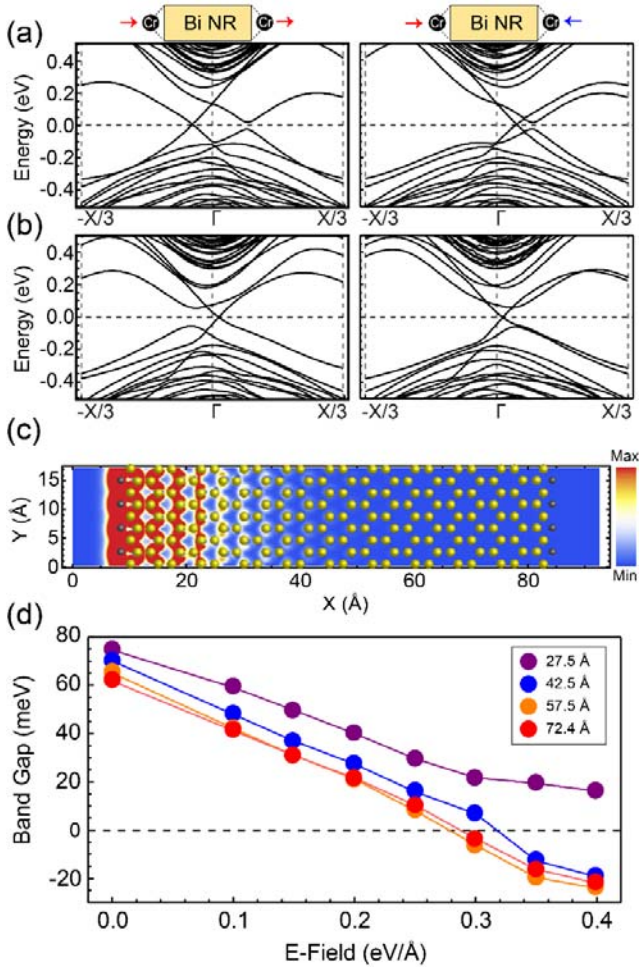

Figure 4 Calculated band structure of Cr-decorated BNR with magnetization (a) in the x-direction and (b) in the z-direction when subjected to an electric field (0.3 V/Å). The magnetic moments on both edges are parallel (left) or antiparallel (right). (c) The squared wave functions of the states near the Fermi level for Cr-decorated BNR with the z-direction magnetization under the electric field (0.3 V/Å). Yellow balls, Bi; Black balls, Cr. (c) The variation of the band gap of Cr-decorated BNR as a function of electric field varying the width of BNR from 27.5 Å to 72. 5 Å.

To find more ways to engineer the edge state, we now investigate the interplay between magnetic interaction and electric field in Cr-decorated BNR. When spins of Cr atoms point to the *x*-direction [Fig. 4(a)] or the *z*-direction [Fig. 4(b)], one of the topological edge states becomes gapped by the *z*-direction electric field of 0.3 V/Å whereas the other still has the linear dispersion without a gap. The selective edge conduction controlled by an

electric field makes it possible to utilize the pure spin-polarized channel as opposed to ordinary topological states where two different chiral channels are juxtaposed. This unique feature is well maintained even if the magnetic moments of both edges are antiparallel to each other [right panels in Figs. 4(a) and (b)]. The magnetic order between both edges just determines the position of the Dirac cone in the momentum space because the width of BNR is thick enough to eliminate the coupling between them [47]. The charge distribution of states near the Fermi level clearly shows the metallic behavior along an edge [Fig. 4(c)]. We note that this unique edge conduction is a universal characteristic of BNR regardless of the type of passivation atoms (Fig. S4) [48]. In addition, the edge-selective conduction always occurs when the width of BNR is larger than ~40 Å [Fig. 4(d)]. Our results imply that tuning of edge conduction through external electric field is efficient and is likely to be feasible if the edge magnetization direction is pinned in the *x*-*z* plane. We also note that, unlike the *z*-direction field, the *x*-direction electric field just makes the Dirac cone at each edge move in the opposite energy directions (Fig. S5) [48].

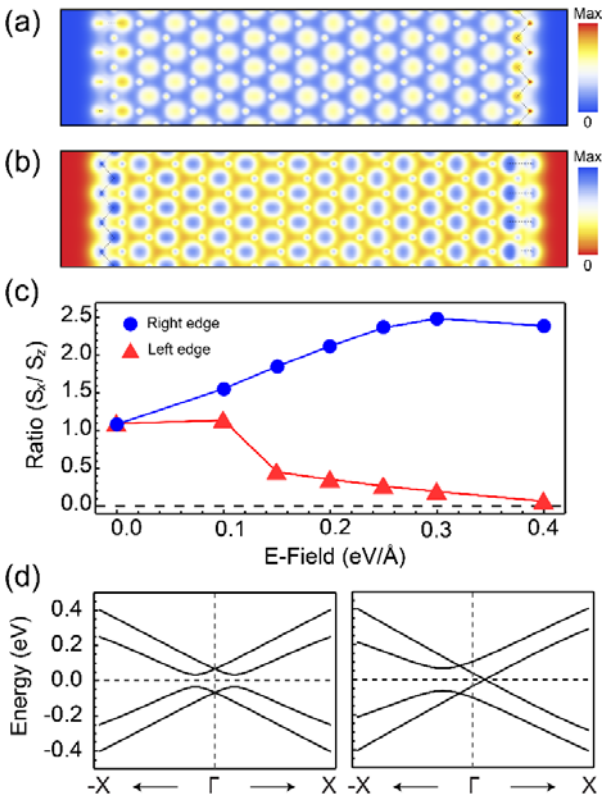

Figure 5 The charge (a) accumulation and (b) depletion induced by an electric field (0.3 V/Å) for Cr-decorated BNR with the z-direction magnetization. (c) The change in the ratio (R) of S_x to S_z as a function of electric field on each edge. (d) Band structures from the model Hamiltonian for R=1 (left) and for R=0 (right).

To understand the underlying physics of this edge-selective conduction, we investigated how the presence of electric field affects the topological edge states. Figs. 5(a) and (b) shows that the charge redistribution of two edges caused by electric field are not identical. In an energetically stable zigzag nanoribbon [17], both edges are not structurally equivalent in the z direction due to its buckled structure and consequently the pattern of charge redistribution also becomes asymmetric under the influence of electric field along the z-direction. This asymmetric charge redistribution leads to different values of λ at the two edges. The variation of the ratio of S_x to S_z upon electric fields of Fig. 5(c) indicates that when BNR is subjected to an external electric field the left and the right edges are dominated by σ_z

and σ_x components, respectively. As explained in Fig. 1, the *z*-direction magnetization acts as a source of mass gap for the σ_x component (right edge) while just shifts the edges state for the σ_z component (left edge). The band structure obtained from our model Hamiltonian shows that the linear Dirac cone is restored by adjusting the spin ratio (R) from R=1 to R=0 [Fig. 5(d)], which confirms the different spin contributions give rise to the edge-selective conduction depending on the direction of electric field.

Ⅳ. SUMMARY

In summary, we show that 1D topological edge states behave differently from 2D surface states under various perturbations such as magnetic doping and external electric field. At the edge, an additional degree of freedom of spin direction whose counterpart does not exist in the surface is allowed and it gives rise to a totally new electronic structure which have never been observed in 2D surface states. Despite the nontrivial Zak phase difference between the magnetic domains, the chiral interface states were not found in our calculations because the topological edge states experience the net magnetic moment in the entire unit cell due to their nonlocal nature. We also propose a way to selectively and reversibly control 1D edge states by applying electric field. Our results shed light on the unexplored magnetized 1D topological states and pave the way for designing a new type of spin device through the edge-selective conduction.

ACKNOWLEDGMENTS

This work was support by the SHINES, an Energy Frontier Research Center founded by the U. S. Department of Energy, Office of Science, Basic Energy Science under Award SC0012670. Calculations were performed on parallel computers at NERSC.

References

[1] K. S. Novoselov, A. K. Geim, S. V. Morozov, D. Jiang, Y. Zhang, S. V. Dubonos, I. V. Grigorieva, and A. A. Firsov, Science **306**, 666 (2004).

[2] B. Radisavljevic, A. Radenovic, J. Brivio, V. Giacometti, and A. Kis, Nat. Nanotechnol. **6**, 147 (2011).

[3] K. S. Novoselov, Z. Jiang, Y. Zhang, S. V. Morozov, H. L. Stormer, U. Zeitler, J. C. Maan, G. S. Boebinger, P. Kim, and A. K. Geim, Science **315**, 1379 (2007).

[4] L. Li, Y. Yu, G. J. Ye, Q. Ge, X. Ou, H. Wu, D. Feng, X. H. Chen, and Y. Zhang, Nat. Nanotechnol. **9**, 372 (2014).

[5] C. Gong, L. Li, Z. Li, H. Ji, A. Stern, Y. Xia, T. Cao, W. Bao, C. Wang, Y. Wang, Z. Q. Qiu, R. J. Cava, S. G. Louie, J. Xia, and X. Zhang, Nature **546**, 265 (2017).

[6] Z. F. Wang, H. Zhang, D. Liu, C. Liu, C. Tang, C. Song, Y. Zhong, J. Peng, F. Li, C. Nie, L. Wang, X. J. Zhou, X. Ma, Q. K. Xue, and F. Liu, Nat. Mater. **15**, 968 (2016).

[7] C. L. Kane, and E. J. Mele, Phys. Rev. Lett. **95**, 226801 (2005).

[8] C. L. Kane, and E. J. Mele, Phys. Rev. Lett. **95**, 146802 (2005).

[9] B. A. Bernevig, T. L. Hughes, and S.-C. Zhang, Science **314**, 1757 (2006).

[10] M. Konig, S. Wiedmann, C. Brune, A. Roth, H. Buhmann, L. W. Molenkamp, X.-L. Qi, and S.-C. Zhang, Science **318**, 766 (2007).

[11] M. Z. Hasan, and C. L. Kane, Rev. Mod. Phys. **82**, 3045 (2010).

[12] H. Wang, S. T. Pi, J. Kim, Z. Wang, H. H. Fu, and R. Q. Wu, Phys. Rev. B **94**, 035112 (2016).

[13] B. Huang, K.-H. Jin, B. Cui, F. Zhai, J. Mei, and F. Liu, Nat. Commun. **8**, 15850 (2017).

[14] V. S. Pribiag, J. A. BeukmanArjan, F. Qu, M. C. Cassidy, C. Charpentier, W. Wegscheider, and L. P. Kouwenhoven, Nat. Nanotechnol. **10**, 593 (2015).

[15] Y. Xu, B. Yan, H.-J. Zhang, J. Wang, G. Xu, P. Tang, W. Duan, and S.-C. Zhang, Phys. Rev. Lett. **111**, 136804 (2013).

[16] X. Qian, J. Liu, L. Fu, and J. Li, Science **346**, 1344 (2014).

[17] K.-H. Jin, and S.-H. Jhi, Phys. Chem. Chem. Phys. **18**, 8637 (2016).

[18] T. Hirahara, G. Bihlmayer, Y. Sakamoto, M. Yamada, H. Miyazaki, S.-i. Kimura, S. Blügel, and S. Hasegawa, Phys. Rev. Lett. **107**, 166801 (2011).

[19] Z. F. Wang, L. Chen, and F. Liu, Nano Lett. **14**, 2879 (2014).

[20] S. Murakami, Phys. Rev. Lett. **97**, 236805 (2006).

[21] L. Chen, Z. F. Wang, and F. Liu, Phys. Rev. B **87**, 235420 (2013).

[22] Z. Liu, C.-X. Liu, Y.-S. Wu, W.-H. Duan, F. Liu, and J. Wu, Phys. Rev. Lett. **107**, 136805 (2011).

[23] M. Wada, S. Murakami, F. Freimuth, and G. Bihlmayer, Phys. Rev. B **83**, 121310 (2011).

[24] F.-C. Chuang, L.-Z. Yao, Z.-Q. Huang, Y.-T. Liu, C.-H. Hsu, T. Das, H. Lin, and A. Bansil, Nano Lett. **14**, 2505 (2014).

[25] S. H. Kim, K.-H. Jin, J. Park, J. S. Kim, S.-H. Jhi, T.-H. Kim, and H. W. Yeom, Phys. Rev. B

89, 155436 (2014).

[26] F. Yang, L. Miao, Z. F. Wang, M.-Y. Yao, F. Zhu, Y. R. Song, M.-X. Wang, J.-P. Xu, A. V. Fedorov, Z. Sun, G. B. Zhang, C. Liu, F. Liu, D. Qian, C. L. Gao, and J.-F. Jia, Phys. Rev. Lett. **109**, 016801 (2012).

[27] N. Kawakami, C.-L. Lin, M. Kawai, R. Arafune, and N. Takagi, Appl. Phys. Lett. **107**, 031602 (2015).

[28] Z.-Q. Huang, F.-C. Chuang, C.-H. Hsu, Y.-T. Liu, H.-R. Chang, H. Lin, and A. Bansil, Phys. Rev. B **88**, 165301 (2013).

[29] F. Reis, G. Li, L. Dudy, M. Bauernfeind, S. Glass, W. Hanke, R. Thomale, J. Schäfer, and R. Claessen, Science **357**, 287 (2017).

[30] K.-H. Jin, and S.-H. Jhi, Sci. Rep. **5**, 8426 (2015).

[31] M. Zhou, W. Ming, Z. Liu, Z. Wang, P. Li, and F. Liu, Proc. Natl. Acad. Sci. U.S.A. **111**, 14378 (2014).

[32] H. Chia-Hsiu, H. Zhi-Quan, C. Feng-Chuan, K. Chien-Cheng, L. Yu-Tzu, L. Hsin, and B. Arun, New J. Phys. **17**, 025005 (2015).

[33] F. Katmis, V. Lauter, F. S. Nogueira, B. A. Assaf, M. E. Jamer, P. Wei, B. Satpati, J. W. Freeland, I. Eremin, D. Heiman, P. Jarillo-Herrero, and J. S. Moodera, Nature **533**, 513 (2016).

[34] W. Liu, L. He, Y. Xu, K. Murata, M. C. Onbasli, M. Lang, N. J. Maltby, S. Li, X. Wang, C. A. Ross, P. Bencok, G. van der Laan, R. Zhang, and K. L. Wang, Nano Lett. **15**, 764 (2015).

[35] M. Li, C.-Z. Chang, B. J. Kirby, M. E. Jamer, W. Cui, L. Wu, P. Wei, Y. Zhu, D. Heiman, J. Li, and J. S. Moodera, Phys. Rev. Lett. **115**, 087201 (2015).

[36] J. Honolka, A. A. Khajetoorians, V. Sessi, T. O. Wehling, S. Stepanow, J. L. Mi, B. B. Iversen, T. Schlenk, J. Wiebe, N. B. Brookes, A. I. Lichtenstein, P. Hofmann, K. Kern, and R. Wiesendanger, Phys. Rev. Lett. **108**, 256811 (2012).

[37] J. Kim, K.-W. Kim, H. Wang, J. Sinova, and R. Wu, Phys. Rev. Lett. **119**, 027201 (2017).

[38] L. Fu, Phys. Rev. Lett. **103**, 266801 (2009).

[39] J. Kim, and S.-H. Jhi, Phys. Rev. B **92**, 104405 (2015).

[40] P. E. Blöchl, Phys. Rev. B **50**, 17953 (1994).

[41] G. Kresse, and D. Joubert, Phys. Rev. B **59**, 1758 (1999).

[42] G. Kresse, and J. Hafner, Phys. Rev. B **47**, 558 (1993).

[43] J. P. Perdew, K. Burke, and M. Ernzerhof, Phys. Rev. Lett. **77**, 3865 (1996).

[44] A. A. Soluyanov, and D. Vanderbilt, Phys. Rev. B **83**, 235401 (2011).

[45] G. Paolo, B. Stefano, B. Nicola, C. Matteo, C. Roberto, C. Carlo, C. Davide, L. C. Guido, C. Matteo, D. Ismaila, C. Andrea Dal, G. Stefano de, F. Stefano, F. Guido, G. Ralph, G. Uwe, G. Christos, K. Anton, L. Michele, M.-S. Layla, M. Nicola, M. Francesco, M. Riccardo, P. Stefano, P. Alfredo, P. Lorenzo, S. Carlo, S. Sandro, S. Gabriele, P. S. Ari, S. Alexander, U. Paolo, and M. W. Renata, J. Phys: Condens. Matter **21**, 395502 (2009).

[46] J. Zak, Phys. Rev. Lett. **62**, 2747 (1989).

[47] J. Kim, S.-H. Jhi, and R. Wu, Nano Lett. **16**, 6656 (2016).

[48] K.-H. Jin, H. W. Yeom, and S.-H. Jhi, Phys. Rev. B **93**, 075308 (2016).